RSC Advances

RSC Advances

www.rsc.org/advances

ROYAL SOCIETY OF CHEMISTRY

www.rsc.org/advances

Bi-axially Oriented Polystyrene/Montmorillonite Nanocomposite Films

Wenhan Huang,[1,2] Songshan Zeng[1], Jingjing Liu[1], Luyi Sun[1,*]

[1]Department of Chemical & Biomolecular Engineering and Polymer Program, Institute of Materials Science, University of Connecticut, Storrs, Connecticut 06269, United States

[2] School of Mechanical and Electrical Engineering, Heyuan Polytechnic, Heyuan, Guangdong 517000, China

*Author to whom correspondence should be addressed:

Dr. Luyi Sun, Tel: (860) 486-6895; Fax: (860) 486-4745; Email: luyi.sun@uconn.edu

Abstract

Polystyrene (PS)/montmorillonite (MMT) nanocomposite films were prepared by bi-axially stretching compounded and extruded PS/MMT nanocomposite sheets, with an aim to achieve intercalation/exfoliation during compounding and an improved level of exfoliation and orientation during stretching. The characterization results support that the expected morphology of improved exfoliation and orientation was achieved, which leads to more significant property improvement compared to the non-stretched nanocomposite sheets. Meanwhile, only marginal deterioration in optical properties was observed in the PS/MMT nanocomposite films. Considering mechanical stretching can be adopted for large scale production, it represents a facile and potential mass production method of nanocomposites for practical applications.

Introduction

Since the pioneering work on nylon-6/montmorillonite (MMT) nanocomposites were reported in early 1990s,[1-3] polymer nanocomposites containing inorganic nanofillers have been well investigated and developed.[4-7] If nanofillers are properly incorporated into a polymer matrix, significant property improvements, including mechanical, barrier, thermal-mechanical, and flame retardant properties are expected at low loading levels.[8-10] New functionalities may also be introduced based on the nature of nanofillers.[11-13]

Although 0-dimenional (0-D) nanoparticles[14-19] and 1-dimensional (1-D) nanofibers/tubes/rods[20-25] have both been well investigated, 2-dimeional (2-D) nanosheets are arguably still the most ideal nanofillers for polymers,[26, 27] particularly for barrier properties improvement.[28] Among a wide variety of 2-D materials, including various clays,[29-40] metal phosphates and phosphonates,[28, 41-52] graphite,[28, 53-60] MMT has remained to be the most popular layered compound in polymer nanocomposite research, mainly because of its low cost,[61] high inherent modulus (~270 GPa),[62] and high aspect ratio.[63] In order to achieve sufficient dispersion of MMT in polymer matrix to obtain desirable properties, MMT is typically treated with organic modifiers to improve its compatibility with monomers/polymers.[6, 64-69]

Polystyrene (PS) nanocomposites have been well explored mainly because of the widespread application of PS.[70-77] PS/MMT nanocomposites typically exhibit moderately improved mechanical and barrier properties.[5, 6, 74] Further improvement of such properties is highly desirable.[78] Based on a sufficient level of dispersion which has already been realized,[6, 64, 65] it would be ideal if one can achieve orientation of MMT nanosheets within a PS matrix for further property enhancement. Orientation of 1-D nanofillers, such as nanotubes and nanofibers, has been explored and achieved.[78-80] Similarly, the orientation of 2-D nanosheets with a high

aspect ratio in a polymer matrix has been investigated because of its significant impact on the final properties of nanocomposites. For example, it is well known that nanocomposites containing exfoliated and oriented clay nanosheets exhibit higher mechanical performance.[33] Furthermore, the nanocomposites containing orientated nanosheets also demonstrate anisotropic mechanical properties with a higher mechanical strength in the orientated direction.[81] For barrier properties, the highly oriented clay nanosheets are much more effective than randomly distributed nanosheets.[81] Such property enhancements may enable PS nanocomposites to compete with certain engineering plastics and thus significantly widening their applications and increasing their values. Thus, it is essential to study the orientation of nanosheets in the polymer matrix. However, much less work has been reported on the orientation of 2-D nanosheets in polymer matrices via conventional processing techniques, mainly owing to the technical challenges.[81, 82] Certain techniques, such as drop casting and layer-by-layer self-assembly have been applied to achieve orientated clay nanosheets in polymer matrix, but such methods are hard to be scaled up for commercial production.[83, 84]

In this research, we aim to prepare PS/MMT nanocomposites via the common compounding approach. Subsequently, the extruded PS/MMT nanocomposite sheets were bi-axially stretched to prepare PS/MMT nanocomposite thin films. The mechanical stretching force may serve two functions: (1) slide the MMT nanosheets (that were intercalated during compounding) apart, which might help separate the MMT nanosheets that were not exfoliated during compounding; (2) align the MMT nanosheets along the stretching direction (film in-plane direction). A higher degree of orientation and an improved level of exfoliation of MMT nanosheets in PS matrix via such a facile mechanical stretching process are expected to effectively improve its physical properties, including stiffness and barrier properties.

4

Experimental

Cloisite[®] 15A, an organically treated MMT (from BYK Additives Inc., USA), was used in this project. It was compounded with a crystal polystyrene (CX5229, Mn: 315,000, polydispersity: 3.5; melt flow rate: 3.0 g/10 min, melt strength: 0.06 N, from Total Petrochemicals USA, Inc.) at a concentration of 5.0 wt% (ca. 2.7 vol%, based on the density of PS[85] of 1.05 g/cm^3 and MMT of 2.01 g/cm^3)[86] on a Leistritz ZSE 50 twin screw extruder. The compounded samples were cast into 1.0 mm sheets on a sheet extruder. The PS/MMT nanocomposite sheets were then stretched on a lab stretcher (Brückner, Germany) at 140 °C to a 6×6 areal draw ratio at a speed of 30 m/min in both machine direction (MD, lengthwise in terms of sheet extrusion) and transverse direction (TD, across the sheet).

X-ray diffraction (XRD) patterns were recorded on a Bruker D5 diffractometer with a graphite monochromator with Cu Kα radiation. Tensile properties (strength, modulus, elongation at break) of all nanocomposite specimens were tested on a universal testing machine (Instron 5869) based on ASTM D 638-99. The transparency of the film samples were characterized on an ultraviolet-visible (UV-Vis) spectrophotometer (VARIAN CARY 5000). For transmission electron microscopy (TEM) characterization, the film samples were embedded into epoxy, which were microtomed into thin slices with a thickness of 80-100 nm on Reichert-Jung Ultracut E ultra-microtome, while the sheet samples were directly microtomed into slices. The thin slices were deposited on 400-mesh copper grids for imaging under an FEI Tecnai T12 S/TEM with an acceleration voltage of 120 kV. Oxygen transmission rates (OTRs) were tested on a MOCON OX-TRAN[®] 1/50 W instruments (ASTM D-3985) at 23 °C and 0% RH. Water vapor transmission rates (WVTRs) were tested on a MOCON PERMATREAN[®] 1/50 W instrument

(ASTM F-1249) at 23 °C and 50% RH. Thermogravimetric analysis was performed using a thermogravimetric analyzer (TGA, TA Instruments Q500) at a heating rate of 10 °C/min under air atmosphere.

Results and Discussion

The main purpose of the mechanical orientation treatment is two folds: (1) potentially slide/split the initially intercalated MMT nanosheets (achieved during compounding) apart, which may help separate the MMT layers that were not exfoliated during compounding; (2) align the dispersed MMT nanosheets with the help of polymer chain orientation, which was exerted by the mechanical stretching force. The entire process is illustrated in Figure 1. As such, a quicker and higher degree of stretching/chain orientation is preferred to achieve a higher degree of exfoliation and orientation of MMT nanosheets. Based on this, in this study, it was attempted to stretch the sheet samples at a relatively low temperature (140 °C, for more effective chain orientation) at a high stretching speed (30 m/min) using the lab stretcher. It was also attempted to stretch the films to a large areal draw ratio. The experiments showed that an areal draw ratio of 6×6 was ideal. An even higher draw ratio led to very thin PS films, usually with defects.
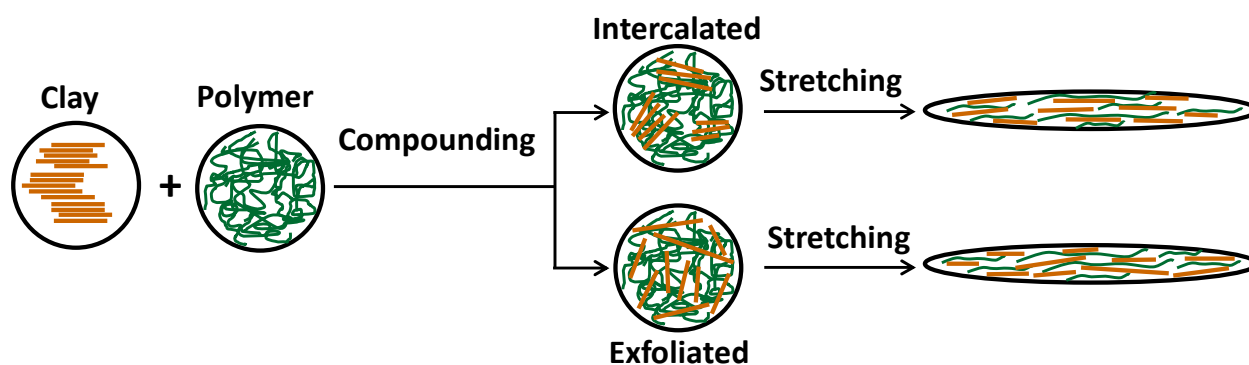

Figure 1. Schematic of the stretch-exfoliation-orientation process.

The morphology of the inorganic nanosheets in polymer matrix is very critical for the resulting performance of the nanocomposites. As shown in Figure 2, in pristine MMT (Cloisite® Na⁺), the interlayer distance is ca. 12.0 Å. After organic modification, Cloisite® 15A exhibited an interlayer distance of 29.6 Å. After being compounded with PS, the diffraction peak of the MMT in the PS/MMT nanocomposite shifted from 2.98° to 2.63°, corresponding to an interlayer distance increase from 29.6 to 33.6 Å. This indicates the intercalation of PS chains into MMT layers in PS/MMT nanocomposite sheet samples, during which the organic modifiers might be partially replaced by PS chains. The existence of this peak also suggests that the layered MMT was not completely exfoliated during the compounding process. After being mechanically stretched into thin films, the film sample exhibited a diffraction peak at ca. 2.68° (33.0 Å). This slight decrease in interlayer distance is expected as during stretching, compression force perpendicular to the stretching (film in-plane) direction was spontaneously generated. The PS chains pre-intercalated into the MMT layers may also be stretched. As a result, the intercalated MMT layers would shrink slightly, leading to a slightly reduced interlayer distance. Meanwhile, the nanocomposite film samples exhibited a slightly less intensive diffraction peak compared to the sheet sample. It is expected that a higher level of exfoliation should be achieved during mechanical stretching process. As such, the diffraction peak should diminish significantly. The reason that this diffraction peak appeared to be more intensive than expected is believed owing to the orientation of nanosheets achieved during the stretching process. The alignment of MMT layers led to preferred orientation along the film in-plane direction, which leads to a higher sensitivity during XRD characterization, thus a more intense peak. Both an enhanced level of exfoliation and orientation is proved in the TEM characterization and will be discussed in detail in the following section.
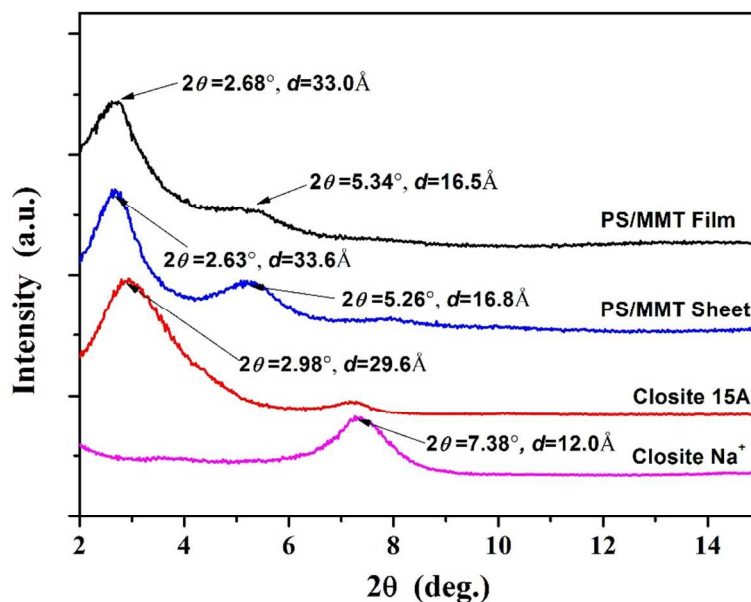
Figure 2. XRD Patterns of PS/MMT nanocomposite films.

TEM characterization offers a direct assessment of the dispersion and orientation of MMT nanosheets in the PS matrix. Figure 3(a-c) presents the TEM images of the PS/MMT nanocomposite sheet sample at various magnifications. It shows that the MMT nanosheets are roughly randomly dispersed in the PS matrix with few appreciable signs of orientation. In principle, extrusion may generate a low level of alignment due to melt flow induced orientation. The reason that such a phenomenon was not observed is probably owing to the relatively large thickness of the extruded sheet sample (1.0 mm) in comparison to the length of MMT nanosheets. Figure 3(b) shows that the layered MMT was partially exfoliated with pristine plate-like shape without breakage. The high magnification TEM image in Figure 3(c) clearly shows that most MMT still consists of multiple layers and some MMT layers were sheared/peeled from the original layered structure, probably by the high shear force during the twin-screw extrusion process. Similar phenomenon was observed by Paul and coworkers. [87-89]

8

After being stretched, the MMT nanosheets in the PS/MMT nanocomposite films exhibited a decent level of orientation as shown in Figure 3(d). This is consistent with the more intense diffraction peak of the film sample as shown in Figure 2. The mechanical stretching force renders the MMT sheets to rotate and align along the stretch direction (SD). Figure 3 also shows that MMT nanosheets exhibit a higher density in the film sample than those in the sheet sample. This phenomenon is exactly expected and is believed simply owing to the sliding/splitting of the MMT nanosheets during the mechanical stretching process. With the help of an image processing software (Nano Measurer version 1.2), the average lateral dimension of the nanosheets as shown in Figure 3e is estimated to be 96±36 nm (Figure 4). Under even higher magnification (Figure 3f), some blur gray shadows were observed around almost each MMT sheet. Such shadows are believed to be contributed by the MMT nanosheets that were split from the original structure, which were tilted and curved and thus out of focus under TEM image. This result supports our hypothesis that the stretching process not only help align MMT nanosheets, but also split some layers out of the MMT layered structure. Such delaminated layers were also roughly oriented along the stretching direction.

Overall, the combined characterization of XRD and TEM suggested that partial exfoliation of MMT was achieved in the bi-axially stretched PS/MMT nanocomposite films. The series of TEM images allow us to visualize the process of the stretch induced nanosheets alignment and delamination in the PS matrix. The alignment and the improved level of exfoliation by the mechanical stretching is believed to be able to effectively improve the mechanical and barrier properties of the formed nanocomposite films, which will be discussed in detail in the following sections.
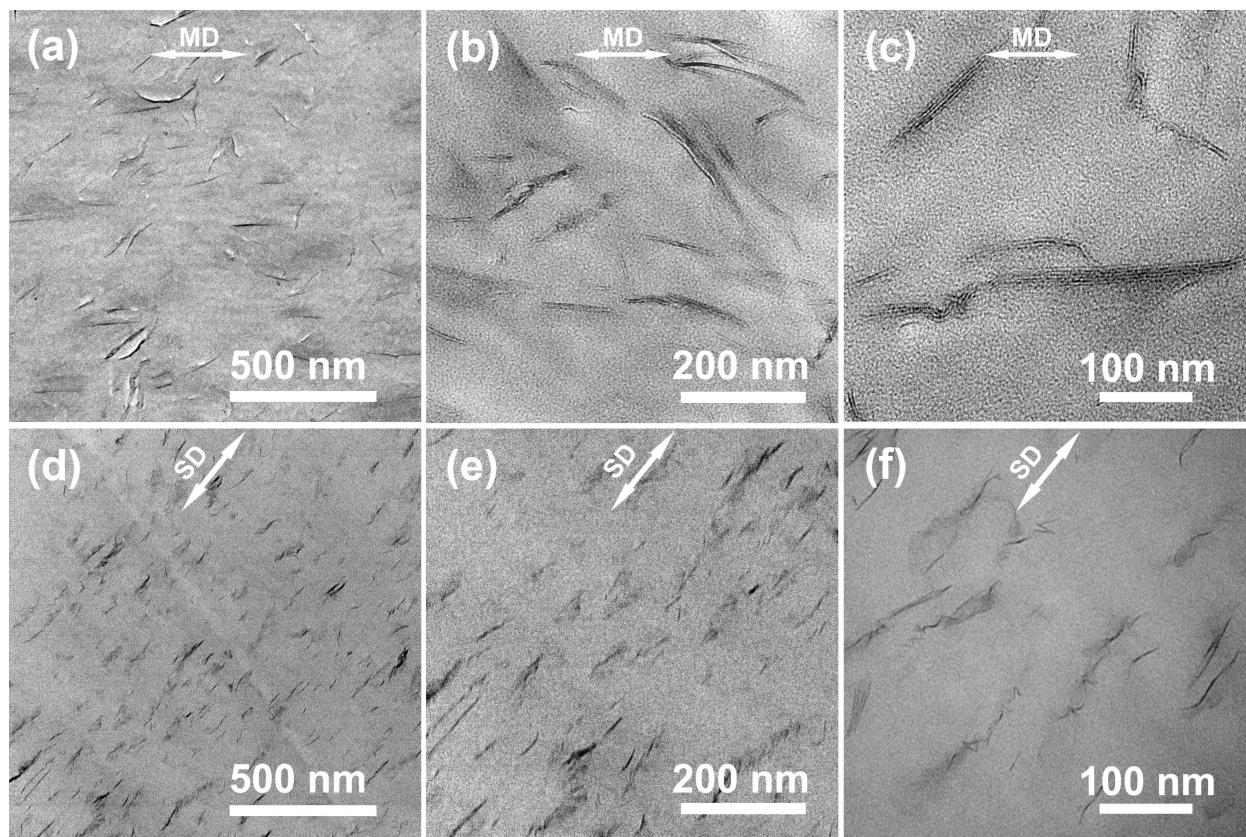
Figure 3. TEM images of the PS/MMT nanocomposite sheet (a-c) and the bi-axially oriented PS/MMT nanocomposite film (d-f) under various magnifications. MD: machine direction during extrusion; SD: stretch direction.
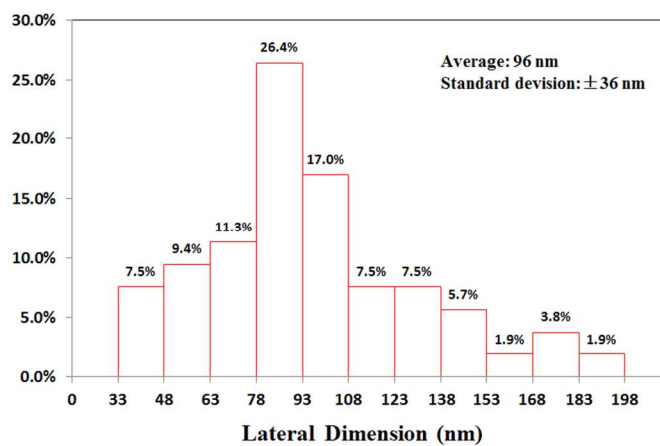

Figure 4. Distribution of the lateral dimension of the MMT nanosheets shown in Figure 3e.

Figure 5 shows the transparency of the neat PS and PS/MMT nanocomposite films with a same thickness of 26 μm. The PS/MMT nanocomposite film can retain a high level of transparency, showing only a marginal decrease in the transmittance, although it contains 5.0 wt% MMT. Overall, the PS/MMT nanocomposite film exhibited outstanding optical transparency along the entire visible spectrum range as demonstrated by both the spectra and the digital picture in Figure 5.
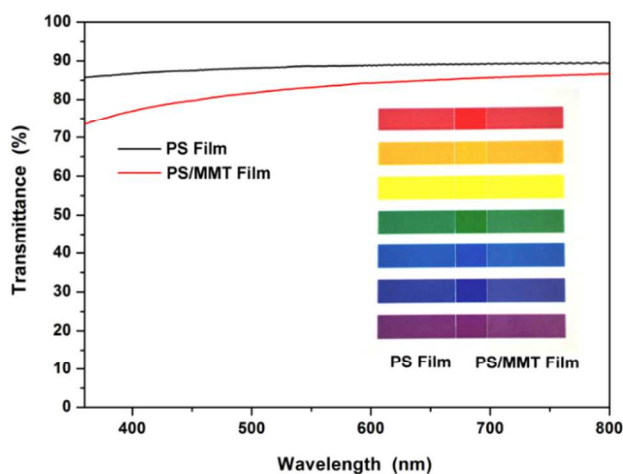

Figure 5. UV-Vis spectra of the neat PS and PS/MMT nanocomposite films. The inset shows a digital picture of a neat PS film (left) and a PS/MMT nanocomposite film (right) placed above a printed rainbow pattern, exhibiting a high transparency along the entire visible spectrum range.

The mechanical testing results (Table 1) show that after bi-axial orientation, both PS and PS nanocomposite film exhibited improved stiffness and strength, which is owing to the polymer chain orientation. With the incorporation of 5.0 wt% MMT, the Young's modulus of the PS/MMT nanocomposite sheet only increased by ca. 4% compared to the neat PS. Meanwhile, its tensile strength and elongation at break decreased. The phenomenon of an increase of modulus and a decrease of strength and elongation is rather common, as polymer nanocomposites tend to be stiffer but more brittle after the incorporation of rigid inorganic nanofillers, which has been reported in the case of PS/laponite and PS/MMT.[90, 91] For the

PS/MMT nanocomposite films, ca. 33% of improvement in Young's modulus was achieved compared to the neat PS film, which is much more significant than the improvement in the PS/MMT nanocomposite sheets (ca. 4%). Meanwhile, a simultaneous improvement in tensile strength (ca. 11%) was also achieved, in contrast to a decrease in tensile strength in the PS/MMT nanocomposite sheets. The elongation at break still deceased but very marginally. The much more significant mechanical property improvements in the PS/MMT nanocomposite films compared to the un-stretched sheets are believed owing to the bi-axial stretching induced orientation and exfoliation of the MMT nanosheets, as shown in Figure 3 and discussed above. Similar results were also reported in fibers and nanotubes reinforced polymer systems.[92] It was reported that the mechanical reinforcement is greatly affected by the orientation and distribution of nanosheets.[93] The split and partially exfoliated MMT nanosheets with exposed edges by the stretching process can increase the interface area between the MMT nanosheets and the PS matrix. The extra interface area can help carry more loads from the PS matrix and thus exhibiting higher mechanical performance. Overall, the results show that the stretching induced delamination and orientation of MMT nanosheets in the PS/MMT nanocomposite films can help effectively enhance the mechanical properties.

Table 1. Mechanical properties of PS and PS/MMT nanocomposite samples.

		Young's Modulus (MPa)	Tensile Strength (MPa)	Elongation at Break (%)
Extruded Sheet (1.0 mm)	PS	1,985 ± 44	34.5 ± 2.0	3.7 ± 0.4
	PS/MMT	2,063 ± 248	31.5 ± 5.0	2.5 ± 0.4
	Improvement	4%	-9%	-32%
Bi-axially Oriented Film (26 μm)	PS	2191 ± 280	73.4 ± 3.6	3.9 ± 0.2
	PS/MMT	2921 ± 151	81.7 ± 5.7	3.6 ± 0.3
	Improvement	33%	11%	-8%

The barrier properties, including WVTR and OTR, of the PS/MMT nanocomposite films are shown in Table 2. The neat PS film (26 μm) exhibited a very high OTR of 7600 cc/(m^2•day) and a moderate WVTR of 20 g/m^2•day. With 5.0 wt% (2.7 vol%) MMT nanosheets, the OTR and WVTR of PS/MMT nanocomposite film were reduced to 5300 cc/(m^2•day) and 10 g/m^2•day, representing a 30% and 50% decrease, respectively. The less effective OTR reduction is probably owing to the high oxygen affinity of PS.[94] While we were not able to prepare a control PS/MMT film sample without MMT orientation for comparison, some literature data (Table 3) show that the PS/MMT nanocomposite film exhibited a more effective barrier property improvement compared to the conventional nanocomposites containing the same or a higher concentration of MMT. Such a much more effective reduction of OTR and WVTR can again be attributed to the MMT nanosheets orientation, in which MMT nanosheets act as impermeable blocks to make the penetration pathway much more tortuous for molecules to travel through.

Table 2. Barrier properties of the PS and PS/MMT nanocomposite films.

Samples	Thickness (μm)	OTR (cc/m^2•day)	Normalized OTR (cc•mm/m^2•day)	WVTR (g/m^2•day)	Normalized WVTR (g•mm /m^2•day)
PS	26	7600	197.6	20	0.52
PS/MMT (2.7 vol%)	26	5300	137.8	10	0.26

Table 3. Literature data of OTR and WVTR reduction of nanocomposites containing MMT.

Samples	Reduction of OTR	Reduction of WVTR
PS/MMT (5.0 wt%) in this report	30%	50%
PS/VDAC/MMT (5 wt%) [95]	8~18%	-
Polyurethanes/MMT (5 wt%) [96]	17~25%	-
Starch/MMT (5 wt%) [97]	-	12~34%
Nylon 6/MMT (10 wt%) [98]	-	15-36%

In order to obtain an even better assessment of the barrier property improvement, the relative permeability data of a nanocomposite containing 2.7 vol% nanosheets with various aspect ratios based on four widely accepted permeation models assuming perfect nanosheet orientation, the Nielsen model,[99] the Cussler model (regular array) ,[100] the Fredrickson-Bicerano model [101], and the Gusev-Lusti model,[102] are plotted in Figure 6. According to Figure 4, the MMT nanosheets in the PS matrix possess an average lateral dimension of 96±36 nm. While it is hard to estimate the thickness of the nanosheets mainly because of the blur shadows as shown in Figure 3f, we assume the MMT nanosheets were perfectly exfoliated into single layers with a thickness of ca. 1.0 nm.[103] Under such a most ideal scenario, the average aspect ratio of the MMT nanosheets could be up to 96±36 (the real average aspect ratio should be lower since some MMT are not completely exfoliated). Based on the above four models as shown in Figure 6, our result is close to three of the models. Since all of the four models are based on perfect sheet orientation, this result indirectly supports that effective orientation and exfoliation has been achieved during the mechanical stretching process.
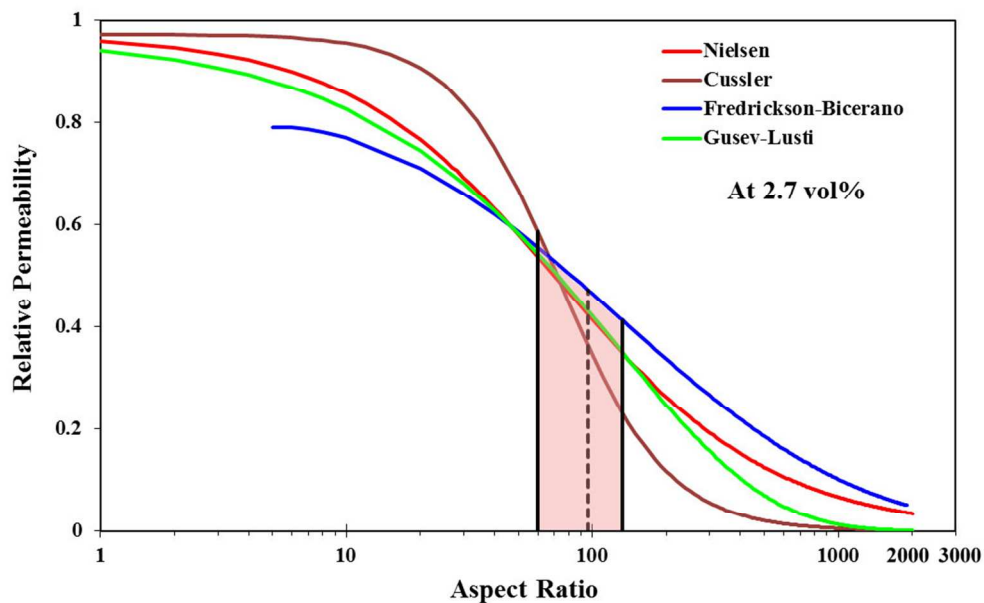
Figure 6. Relative permeability of polymer nanocomposites estimated by various models.

Similar to the barrier properties, the PS/MMT nanocomposite films exhibited a higher thermal stability than the neat PS film, mainly owing to the effective blocking of heat transfer and oxygen permeation by the MMT nanosheets. The TGA thermograms in Figure 7 clearly show the improvement of the thermal stability of PS after the addition of MMT nanosheets. For the neat PS film, the 10% thermal induced weight loss occurred at ca. 325 °C, which it was 343 °C for the PS/MMT nanocomposite film.

Figure 7. TGA thermograms of the neat PS and PS/MMT nanocomposite films.
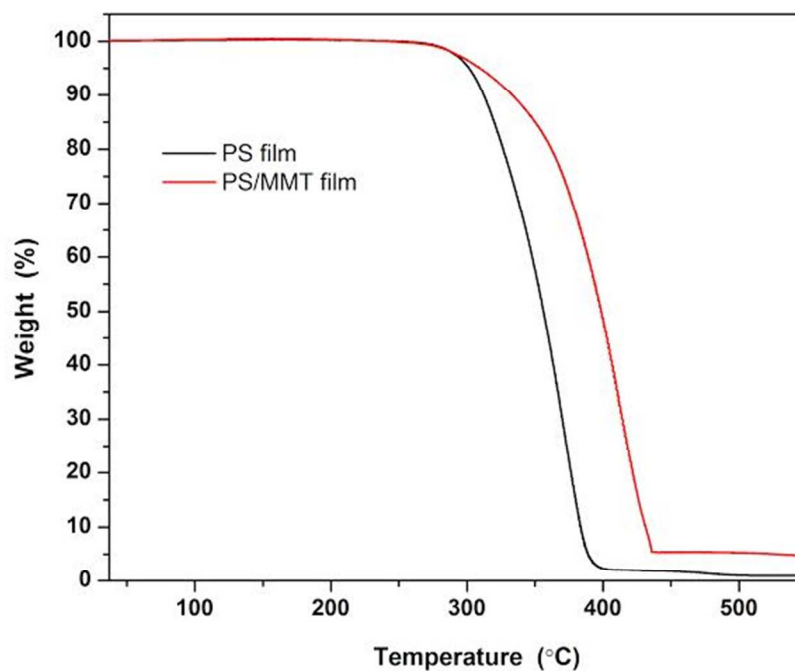
Conclusions

PS/MMT nanocomposite films were prepared by bi-axially stretching the compounded and extruded sheet samples. The TEM and XRD characterization results show that both orientation and exfoliation of MMT nanosheets were improved by mechanical stretching. Overall, partial exfoliation has been achieved during this very facile process. The characterization data show that the PS/MMT nanocomposite films exhibit much more significant improvement in terms of both mechanical and gas barrier properties than the non-stretched PS/MMT nanocomposite sheet samples. Such more effective property improvements are believed owing to the nanosheet orientation and exfoliation induced by stretching. Considering mechanical stretching can be adopted for large scale production, it represents a facile and potential mass production method of nanocomposites for practical applications.

16

Acknowledgements

References:

1. A. Usuki, Y. Kojima, M. Kawasumi, A. Okada, Y. Fukushima, T. Kurauchi and O. Kamigaito, *Journal of Materials Research*, 1993, 8, 1179-1184.
2. Y. Kojima, A. Usuki, M. Kawasumi, A. Okada, Y. Fukushima, T. Kurauchi and O. Kamigaito, *Journal of Materials Research*, 1993, 8, 1185-1189.
3. Y. Kojima, A. Usuki, M. Kawasumi, A. Okada, T. Kurauchi and O. Kamigaito, *Journal of Polymer Science, Part A: Polymer Chemistry*, 1993, 31, 983-986.
4. G. Choudalakis and A. D. Gotsis, *European Polymer Journal*, 2009, 45, 967-984.
5. J. Jordan, K. I. Jacob, R. Tannenbaum, M. A. Sharaf and I. Jasiuk, *Materials Science and Engineering: A*, 2005, 393, 1-11.
6. S. Sinha Ray and M. Okamoto, *Progress in Polymer Science*, 2003, 28, 1539-1641.
7. S. Zeng, C. Reyes, J. Liu, P. A. Rodgers, S. H. Wentworth and L. Sun, *Polymer*, 2014, 55, 6519-6528.
8. A. Okada and A. Usuki, *Macromolecular Materials and Engineering*, 2006, 291, 1449-1476.
9. Y. MAi and Z. YU, *Physical Properties and Applications of Polymer Nanocomposites*, 2010, 347.
10. E. A. Stefanescu, *Recent Patents on Materials Science*, 2010, 3, 1-12.
11. P. Pissis, S. Kripotou and A. Kyritsis, in *Physical Properties and Applications of Polymer Nanocomposites*, eds. S. C. Tjong and Y. W. Mai, Woodhead Publishing, 2010, DOI: http://dx.doi.org/10.1533/9780857090249.2.247, pp. 247-279.
12. M. Factor and S. Lee, *Particle Technology and Applications*, 2012, 235.
13. A. B. Morgan and J. Gilman, *Mater. Matters*, 2007, 2, 20-25.
14. J. H. Park, Y. T. Lim, O. O. Park, J. K. Kim, J.-W. Yu and Y. C. Kim, *Chemistry of Materials*, 2004, 16, 688-692.
15. N. Nakayama and T. Hayashi, *Polymer Degradation and Stability*, 2007, 92, 1255-1264.
16. T. Kashiwagi, F. Du, J. F. Douglas, K. I. Winey, R. H. Harris and J. R. Shields, *Nat Mater*, 2005, 4, 928-933.
17. C. Xiang, Y. Zou, L.-X. Sun and F. Xu, *Sensors and Actuators B: Chemical*, 2009, 136, 158-162.
18. N. Cioffi, L. Torsi, N. Ditaranto, G. Tantillo, L. Ghibelli, L. Sabbatini, T. Bleve-Zacheo, M. D'Alessio, P. G. Zambonin and E. Traversa, *Chemistry of Materials*, 2005, 17, 5255-5262.
19. M. K. Corbierre, N. S. Cameron, M. Sutton, K. Laaziri and R. B. Lennox, *Langmuir*, 2005, 21, 6063-6072.
20. B. Pradhan, K. Setyowati, H. Liu, D. H. Waldeck and J. Chen, *Nano Letters*, 2008, 8, 1142-1146.
21. F. Du, R. C. Scogna, W. Zhou, S. Brand, J. E. Fischer and K. I. Winey, *Macromolecules*, 2004, 37, 9048-9055.
22. Y. Ye, H. Chen, J. Wu and L. Ye, *Polymer*, 2007, 48, 6426-6433.
23. M. Du, B. Guo and D. Jia, *Polymer International*, 2010, 59, 574-582.
24. K. Hedicke-Höchstötter, G. T. Lim and V. Altstädt, *Composites Science and Technology*, 2009, 69, 330-334.
25. K. Prashantha, H. Schmitt, M. F. Lacrampe and P. Krawczak, *Composites Science and Technology*, 2011, 71, 1859-1866.

26.   A. V. Murugan, T. Muraliganth and A. Manthiram, *Chemistry of Materials*, 2009, 21, 5004-5006.

27.   G. Chen, C. Wu, W. Weng, D. Wu and W. Yan, *Polymer*, 2003, 44, 1781-1784.

28.   L. Sun and H.-J. Sue, in *Barrier Properties of Polymer Clay Nanocomposites*, ed. V. Mittal, Nova Science Publishers, New York, USA, 2010, pp. 73-93.

29.   L. Sun, W. J. Boo, J. Liu, C.-W. Tien, H.-J. Sue, M. J. Marks and H. Pham, *Polymer Engineering and Science*, 2007, 47, 1708-1714.

30.   J. W. Gilman, *Applied Clay Science*, 1999, 15, 31-49.

31.   M. Okamoto, S. Morita and T. Kotaka, *Polymer*, 2001, 42, 2685-2688.

32.   C. D. Muzny, B. D. Butler, H. J. M. Hanley, F. Tsvetkov and D. G. Peiffer, *Materials Letters*, 1996, 28, 379-384.

33.   T. Lan, P. D. Kaviratna and T. J. Pinnavaia, *Chemistry of Materials*, 1995, 7, 2144-2150.

34.   E. P. Giannelis, R. Krishnamoorti and E. Manias, in *Polymers in Confined Environments*, eds. S. Granick, K. Binder, P. G. de Gennes, E. P. Giannelis, G. S. Grest, H. Hervet, R. Krishnamoorti, L. Léger, E. Manias, E. Raphaël and S. Q. Wang, Springer Berlin Heidelberg, 1999, vol. 138, ch. 3, pp. 107-147.

35.   M. Okamoto, S. Morita, H. Taguchi, Y. H. Kim, T. Kotaka and H. Tateyama, *Polymer*, 2000, 41, 3887-3890.

36.   T. Lan and T. J. Pinnavaia, *Chemistry of Materials*, 1994, 6, 2216-2219.

37.   N. Sheng, M. C. Boyce, D. M. Parks, G. C. Rutledge, J. I. Abes and R. E. Cohen, *Polymer*, 2004, 45, 487-506.

38.   K. J. Yao, M. Song, D. J. Hourston and D. Z. Luo, *Polymer*, 2002, 43, 1017-1020.

39.   M. Alexandre and P. Dubois, *Materials Science and Engineering: R: Reports*, 2000, 28, 1-63.

40.   S. Horsch, G. Serhatkulu, E. Gulari and R. M. Kannan, *Polymer*, 2006, 47, 7485-7496.

41.   H.-J. Sue, K. T. Gam, N. Bestaoui, N. Spurr and A. Clearfield, *Chemistry of Materials*, 2004, 16, 242-249.

42.   H.-J. Sue, K. T. Gam, N. Bestaoui, A. Clearfield, M. Miyamoto and N. Miyatake, *Acta Materialia*, 2004, 52, 2239-2250.

43.   L. Sun, W. J. Boo, D. Sun, A. Clearfield and H.-J. Sue, *Chemistry of Materials*, 2007, 19, 1749-1754.

44.   W. J. Boo, L. Sun, J. Liu, A. Clearfield and H.-J. Sue, *Journal of Physical Chemistry C*, 2007, 111, 10377-10381.

45.   W. J. Boo, L. Sun, J. Liu, A. Clearfield, H.-J. Sue, M. J. Mullins and H. Pham, *Composites Science and Technology*, 2007, 67, 262-269.

46.   W. J. Boo, L. Sun, J. Liu, E. Moghbelli, A. Clearfield, H.-J. Sue, H. Pham and N. Verghese, *Journal of Polymer Science, Part B: Polymer Physics*, 2007, 45, 1459-1469.

47.   W. J. Boo, L. Sun, G. L. Warren, E. Moghbelli, H. Pham, A. Clearfield and H.-J. Sue, *Polymer*, 2007, 48, 1075-1082.

48.   L. Sun, W. J. Boo, A. Clearfield, H.-J. Sue and H. Q. Pham, *Journal of Membrane Science*, 2008, 318, 129-136.

49.   L. Sun, W.-J. Boo, J. Liu, A. Clearfield, H.-J. Sue, N. E. Verghese, H. Q. Pham and J. Bicerano, *Macromolecular Materials and Engineering*, 2009, 294, 103-113.

50.   E. Moghbelli, L. Sun, H. Jiang, W. J. Boo and H.-J. Sue, *Polymer Engineering and Science*, 2009, 49, 483-490.

51. L. Sun, J. Liu, S. R. Kirumakki, E. D. Schwerdtfeger, R. J. Howell, K. Al-Bahily, S. A. Miller, A. Clearfield and H.-J. Sue, *Chemistry of Materials*, 2009, 21, 1154-1161.
52. S. Wei, M. Lizu, X. Zhang, J. Sampathi, L. Sun and M. F. Milner, *High Performance Polymers*, 2013, 25, 25-32.
53. G.-H. Chen, D.-J. Wu, W.-G. Weng and W.-L. Yan, *Journal of Applied Polymer Science*, 2001, 82, 2506-2513.
54. Y.-X. Pan, Z.-Z. Yu, Y.-C. Ou and G.-H. Hu, *Journal of Polymer Science Part B: Polymer Physics*, 2000, 38, 1626-1633.
55. X. S. Du, M. Xiao and Y. Z. Meng, *European Polymer Journal*, 2004, 40, 1489-1493.
56. K. P. Pramoda, H. Hussain, H. M. Koh, H. R. Tan and C. B. He, *Journal of Polymer Science Part A: Polymer Chemistry*, 2010, 48, 4262-4267.
57. Z. Song, T. Xu, M. L. Gordin, Y.-B. Jiang, I.-T. Bae, Q. Xiao, H. Zhan, J. Liu and D. Wang, *Nano Letters*, 2012, 12, 2205-2211.
58. H.-B. Zhang, W.-G. Zheng, Q. Yan, Y. Yang, J.-W. Wang, Z.-H. Lu, G.-Y. Ji and Z.-Z. Yu, *Polymer*, 2010, 51, 1191-1196.
59. X. Yang, L. Li, S. Shang and X.-m. Tao, *Polymer*, 2010, 51, 3431-3435.
60. J. R. Potts, D. R. Dreyer, C. W. Bielawski and R. S. Ruoff, *Polymer*, 2011, 52, 5-25.
61. S. M. Lloyd and L. B. Lave, *Environmental Science & Technology*, 2003, 37, 3458-3466.
62. O. L. Manevitch and G. C. Rutledge, *Journal of Physical Chemistry B*, 2004, 108, 1428-1435.
63. J. L. Suter, P. V. Coveney, H. C. Greenwell and M.-A. Thyveetil, *The Journal of Physical Chemistry C*, 2007, 111, 8248-8259.
64. F. B. Barlas, D. Ag Seleci, M. Ozkan, B. Demir, M. Seleci, M. Aydin, M. A. Tasdelen, H. M. Zareie, S. Timur, S. Ozcelik and Y. Yagci, *Journal of Materials Chemistry B*, 2014, 2, 6412-6421.
65. T. Agag and T. Takeichi, *Polymer*, 2000, 41, 7083-7090.
66. G. Xu, S. Qin, J. Yu, Y. Huang, M. Zhang and W. Ruan, *RSC Advances*, 2015, 5, 29924-29930.
67. C.-W. Chiu and J.-J. Lin, *Progress in Polymer Science*, 2012, 37, 406-444.
68. C.-W. Chiu, T.-K. Huang, Y.-C. Wang, B. G. Alamani and J.-J. Lin, *Progress in Polymer Science*, 2014, 39, 443-485.
69. M. R. DashtArzhandi, A. F. Ismail and T. Matsuura, *RSC Advances*, 2015, 5, 21916-21924.
70. M. Xiao, L. Sun, J. Liu, Y. Li and K. Gong, *Polymer*, 2002, 43, 2245-2248.
71. X. L. Chen, S. Y. Wei, C. Gunesoglu, J. H. Zhu, C. S. Southworth, L. Y. Sun, A. B. Karki, D. P. Young and Z. H. Guo, *Macromolecular Chemistry and Physics*, 2010, 211, 1775-1783.
72. X. Yan, Q. He, X. Zhang, H. Gu, H. Chen, Q. Wang, L. Sun, S. Wei and Z. Guo, *Macromolecular Materials and Engineering*, 2014, 299, 485-494.
73. J. L. Vickery, A. J. Patil and S. Mann, *Advanced Materials*, 2009, 21, 2180-2184.
74. D. R. Paul and L. M. Robeson, *Polymer*, 2008, 49, 3187-3204.
75. L. J. Cote, R. Cruz-Silva and J. Huang, *Journal of the American Chemical Society*, 2009, 131, 11027-11032.
76. O. C. Compton, S. W. Cranford, K. W. Putz, Z. An, L. C. Brinson, M. J. Buehler and S. T. Nguyen, *ACS Nano*, 2011, 6, 2008-2019.

77. K. Wakabayashi, P. J. Brunner, J. i. Masuda, S. A. Hewlett and J. M. Torkelson, *Polymer*, 2010, 51, 5525-5531.
78. H. Wang, H. Zhang, W. Zhao, W. Zhang and G. Chen, *Composites Science and Technology*, 2008, 68, 238-243.
79. X. Q. Chen, T. Saito, H. Yamada and K. Matsushige, *Applied Physics Letters*, 2001, 78, 3714-3716.
80. P. V. Kamat, K. G. Thomas, S. Barazzouk, G. Girishkumar, K. Vinodgopal and D. Meisel, *Journal of the American Chemical Society*, 2004, 126, 10757-10762.
81. L. S. Loo and K. K. Gleason, *Polymer*, 2004, 45, 5933-5939.
82. P. Nawani, C. Burger, L. Rong, B. Chu, B. S. Hsiao, A. H. Tsou and W. Weng, *Polymer*, 2010, 51, 5255-5266.
83. P. Podsiadlo, A. K. Kaushik, E. M. Arruda, A. M. Waas, B. S. Shim, J. Xu, H. Nandivada, B. G. Pumplin, J. Lahann, A. Ramamoorthy and N. A. Kotov, *Science*, 2007, 318, 80-83.
84. T. Verho, M. Karesoja, P. Das, L. Martikainen, R. Lund, A. Alegría, A. Walther and O. Ikkala, *Advanced Materials*, 2013, 25, 5055-5059.
85. M. Godin, A. K. Bryan, T. P. Burg, K. Babcock and S. R. Manalis, *Applied Physics Letters*, 2007, 91, 123121.
86. A. Usuki, Y. Kojima, M. Kawasumi, A. Okada, Y. Fukushima, T. Kurauchi and O. Kamigaito, *Journal of Materials Research*, 1993, 8, 1179-1184.
87. F. Chavarria, K. Nairn, P. White, A. J. Hill, D. L. Hunter and D. R. Paul, *Journal of Applied Polymer Science*, 2007, 105, 2910-2924.
88. F. Chavarria and D. R. Paul, *Polymer*, 2006, 47, 7760-7773.
89. F. Chavarria and D. R. Paul, *Polymer*, 2004, 45, 8501-8515.
90. R. Ruggerone, C. J. G. Plummer, N. Negrete Herrera, E. Bourgeat-Lami and J. A. E. Månson, *Engineering Fracture Mechanics*, 2009, 76, 2846-2855.
91. P. Uthirakumar, M.-K. Song, C. Nah and Y.-S. Lee, *European Polymer Journal*, 2005, 41, 211-217.
92. B. S. Retnam, M. Sivapragash and P. Pradeep, *Bulletin of Materials Science*, 2014, 37, 1059-1064.
93. R. McCardle, S. Fakirov and D. Bhattacharyya, *Macromolecular Symposia*, 2013, 327, 64-71.
94. E. Dunkerley and D. Schmidt, *Macromolecules*, 2010, 43, 10536-10544.
95. S. Nazarenko, P. Meneghetti, P. Julmon, B. G. Olson and S. Qutubuddin, *Journal of Polymer Science Part B: Polymer Physics*, 2007, 45, 1733-1753.
96. M. A. Osman, V. Mittal, M. Morbidelli and U. W. Suter, *Macromolecules*, 2003, 36, 9851-9858.
97. X. Tang, S. Alavi and T. J. Herald, *Cereal Chemistry Journal*, 2008, 85, 433-439.
98. E. Picard, A. Vermogen, J. F. Gérard and E. Espuche, *Journal of Membrane Science*, 2007, 292, 133-144.
99. L. E. Nielsen, *Journal of Macromolecular Science—Chemistry*, 1967, 1, 929-942.
100. N. K. Lape, E. E. Nuxoll and E. Cussler, *Journal of Membrane Science*, 2004, 236, 29-37.
101. S. Takahashi, H. Goldberg, C. Feeney, D. Karim, M. Farrell, K. O'leary and D. Paul, *Polymer*, 2006, 47, 3083-3093.
102. A. A. Gusev and H. R. Lusti, *Advanced Materials*, 2001, 13, 1641.

103.   E. P. Giannelis, *Advanced Materials*, 1996, 8, 29-35.